

DADA: A Large-scale Benchmark and Model for Driver Attention Prediction in Accidental Scenarios

Jianwu Fang^{1,2}, Dingxin Yan¹, Jiahuan Qiao¹, and Jianru Xue²

Abstract—Driver attention prediction has recently absorbed increasing attention in traffic scene understanding and is prone to be an essential problem in vision-centered and human-like driving systems. This work, different from other attempts, makes an attempt to predict the driver attention in accidental scenarios containing normal, critical and accidental situations simultaneously. However, challenges tread on the heels of that because of the dynamic traffic scene, intricate and imbalanced accident categories. With the hypothesis that driver attention can provide a selective role of crash-object¹ for assisting driving accident detection or prediction, this paper designs a multi-path semantic-guided attentive fusion network (MSAFNet) that learns the spatio-temporal semantic and scene variation in prediction. For fulfilling this, a large-scale benchmark with 2000 video sequences (named as DADA-2000) is contributed with laborious annotation for driver attention (fixation, saccade, focusing time), accident objects/intervals, as well as the accident categories, and superior performance to state-of-the-arts are provided by thorough evaluations. As far as we know, this is the first comprehensive and quantitative study for the human-eye sensing exploration in accidental scenarios. DADA-2000 is available at <https://github.com/JWFangit/LOTVS-DADA>.

Index Terms—Driver attention prediction, Benchmark, Accidental scenarios, Driving accident prediction

I. INTRODUCTION

WARNING: There may be an accident in 5 seconds. This warning is undoubtedly helpful and expected when driving, which releases enough time to control the vehicle to avoid a collision. Some previous investigations conclude that the main factor for causing road fatalities is the absence of driver attention [1], [2], including the distracted driving [3]², drowsy driving, drunk driving, etc. However, accidents having the long-tail characteristic of traffic scene are rather difficult to be predicted while should be avoided with top priority as early as possible for facilitating safe driving. Consequently, it is promising to learn the sober human-focusing experience being exposed to accidental scenarios to give a warning of crash-objects for autonomous driving or assisted driving systems, named as driver attention prediction in driving accidents (DADA). In the meanwhile, driver attention is the vital way to interact with surroundings [4], which commonly shows quick identification for the crucially visual objects or regions (e.g.,



Fig. 1. Examples of driver attention prediction results on two typical crossing situations by some state-of-the-art methods, i.e., DR(eye)VE [13], BDDA [14], ACLNet [15] and the proposed approach.

foveal vision [5]) in the crowd traffic scene, and helps to search a safe routine to the location wanting to go.

Driver attention has been noticed and studied for decades, and commonly formulated as searching the selective road participants or routine guidance points in driving situations [6]–[8]. For a long time, these studies were investigated by a variety of physiological experiments [9], [10] for fatigue detection [11], illumination adaptation, object searching, etc., and are venerable to the highly subjective differences between drivers because of the distinct driving habits, driving experience, age, gender, culture, and so on [4], [12]. Moreover, these experiments usually need contact-type equipments to collect the attention data, and difficult to be implemented in large scale. Consequently, it is hard to obtain a convincing knowledge to help the driver attention prediction in diverse and different driving situations.

Recently, some efforts began to formulate the driver attention prediction as computer vision techniques, and gathered attention data of drivers on large-scale images and videos [13], [14], [16], [17]. For instances, the recent DR(eye)VE project [13] comprising of 555,000 frames collected the driver attention in a car (named as in-car collection) mounted eye-tracker equipments. Nevertheless, the scenarios in DR(eye)VE are sunny and unobstructed, and exposed by one driver's view in attention collection. In view of this, Berkley Deep Drive laboratory launched a driver attention prediction project (BDDA) in critical situations with braking events [14]. Differently, because of the rather rarity of critical situations, they collected the attention data in laboratory (named as in-lab

¹J. Fang, D. Yan, and J. Qiao are with the School of Electronic and Control Engineering, Chang'an University, Xi'an, China; J. Fang is also with the Institute of Artificial Intelligence and Robotics, Xi'an Jiaotong University, Xi'an, China fangjianwu@chd.edu.cn.

²J. Xue is with the Institute of Artificial Intelligence and Robotics, Xi'an Jiaotong University, Xi'an, China jrxue@mail.xjtu.edu.cn.

¹Crash-object in this paper denotes the objects that will occur accidents.

²<https://crashstats.nhtsa.dot.gov/Api/Public/ViewPublication/812700>

collection), and claimed that in-lab collection is better than in-car collection owing to that observers are more focused without the disturbance of surroundings and extra maneuvers for controlling cars. BDDA is most related to our work, while did not consider the driver attention characteristics in actual and more rarely accidental situations in driving. Certainly, to be clear, each video sequence in this work not only contains the accidents, but also owns the normally and critically temporal frames before and after the accidents. In other words, we focus on the driver attention prediction in normal, critical, and accidental situations simultaneously.

To fulfill this goal, we constructed a large-scale benchmark with 2000 video sequences (called DADA-2000, with over 650,000 frames), laboriously annotated the driver attention (fixation, saccade, focusing time), accident objects/intervals, as well as 54 accident categories by 20 observers. Following BDDA, we also carefully annotated the attention data in lab on various scenes with diverse weather conditions (sunny, snowy, and rainy), light conditions (daytime and nighttime), occasions (highway, urban, rural, and tunnel), and different accident categories.

Furthermore, we propose a multi-path semantic attentive fusion network (MSAFNet) for driver attention prediction, consisting of a multi-path of 3D encoding module (M3DE), semantic-guided attentive fusion module (SAF) and a driver attention map decoding module (DAMD). M3DE extends the 3D convolution with multiple interleaved 3D blocks, such as 3D convolution, 3D batch normalization and 3D pooling. SAF aims to explore the semantic variation in the driver attention prediction, and achieve the spatio-temporal dynamics transition by attentive fusion of convolutional-LSTM (convLSTM). MSAFNet is comprehensively compared with 7 state-of-the-art approaches, and superior performance is obtained, as demonstrated in Fig. 1.

In brief, the contributions of this work are three-fold.

- A large-scale benchmark called DADA-2000 concentrating on the driver attention prediction in accidental scenarios is built, which has 2000 video sequences with over 650,000 frames carefully collected the eye-tracking data (fixation, saccade, and focusing time) of 20 observers, annotated 54 kinds of accident categories, and accidental object/intervals. The statistics of DADA-2000 is comprehensively analyzed. As far as we know, DADA-2000 is the first dataset concentrating the driver attention prediction in accidental situations, and covers more diverse and complex scenarios than previous ones.
- An multi-path semantic-guided attentive fusion network is proposed to learn both the semantic and vision variations in driver attention prediction, where the spatio-temporally hidden representation of vision and semantics are robustly learned, and the spatio-temporal dynamics transition over the frames of the given video clip are fulfilled by attentive fusion of convolutional-LSTM (convLSTM).
- We demonstrate superior performance of the proposed method against 7 state-of-the-art approaches on different behavior types in accidental scenarios and overall dataset. Moreover, we give an study for the comparison on the

average delayed frames (ADF) ahead or behind the starting boundary of accident window between human-eye focusing and the proposed driver attention predictor in the experiments, which reflects the capability of humans and our model for early accident prediction.

This work is the extended version of our ITSC2019 [18], while has following differences. We make more detailed analysis on our DADA-2000 benchmark, and give the analysis on the average delayed frames (ADF) ahead or behind the starting boundary of accidents where the crash-object were firstly noticed by human eyes. By that, we can conclude that which kind of accident can be predicted early by driver attention. A novel driver attention prediction model is proposed which learns the semantic and vision variation in prediction, and fulfilled by an attentive conv-LSTM fusion module. We provide a comparative study on DADA-2000 benchmark with thorough evaluations between the proposed method with 7 state-of-the-art approaches.

The rest of the this paper is organized as follows. Section II briefly reviews the related literatures to this work. Section III analyzes the statistics of DADA-2000, and Section IV presents the proposed multi-path semantic-guided attentive fusion network. Section V provides the extensive experiments and analysis, and the final conclusion and future work are given in Section VI.

II. RELATED WORK

This work is closely related to the dynamic visual attention prediction in general videos and driver attention prediction, as briefly discussed in the following subsections.

A. Dynamic Visual Attention Prediction

Dynamic visual attention prediction aims to quantitatively localize the most attractive regions in videos by human eyes, commonly producing a 2D saliency map allocating the likelihood on the locations attracting the dynamic fixations [19]–[22]. By that, it is testable to understand the dynamic human eye-gazing pattern at behavioral and neural levels. Generally, similar to the extensively interested study on static images, dynamic human fixation prediction in the previous research can be categorized as top-down methods (i.e., task-specific) and bottom-up approaches (i.e., task-agnostic). Top-down formulations often find the most relevant regions to a specific ongoing task and goal [23], which often entails supervised learning with pre-collected task labels by a large set of training examples, and varies in different environments. Bottom-up mechanism commonly detects the salient piece of information in a free-viewing mode [24]. Among these two categories, bottom-up models were extensively studied and excavated the distinctive information representation of region of interests in free-viewing in photometrical (color, texture, contrast, depth, motion, flicker, etc.), geometrical (symmetry, connectivity, vanishing point, center-bias, object center-bias, etc.), psychophysical (surprise, emotional valence, interestingness, objectness, etc.), psychological (the principles in Gestalt) and social cues (culture, gender, gazing habit, signs, text, faces, etc.).

Compared with the significantly interested visual attention researches for static images, the less studied dynamic visual attention prediction concentrates more on motion or object correlations in temporal frames [21], [22], [25]–[28]. With the help of the development of deep learning and the large-scale annotated database for dynamic visual attention prediction, such as Hollywood-2 [29], UCF sports [29], DIEM [30], LEDOV [22], DHF1K [15], etc., this field is promoted with a large jump in performance. For instance, Jiang *et al.* [22] proposed a saliency-structured convolutional long short-term memory (SS-ConvLSTM) model which considered the spatial center-surround bias and temporal attention transmission over frames. Wang *et al.* [15] designed an attentive CNN-LSTM model to learn the spatial and temporal scene representations in prediction. The work [31] designed a multi-stream fusion network, called spatio-temporal saliency networks, investigated different fusion mechanisms to spatial and temporal information integration. Recent dynamic visual attention prediction methods exploited the stimuli from RGB videos and focused the motion clue largely, rare work considered the semantic information within the videos. As for driving scenarios, semantic variation shows significant role for safe driving, especially for the accidental scenarios often appearing the crash-object suddenly. Therefore, we introduce the semantic variation of traffic scene to serve driver attention prediction in accidental scenarios.

B. Driver Attention Prediction

Drivers can quickly identify the important visual cues and objects influencing their driving intention in the blurry periphery vision and then make eye movements to direct their more accurate foveal vision to the important regions [8], [32]. Driver attention is the direct window to understand the driver behavior and intention in different driving situations [6], [7]. Over decades, safety of self-driving cars has been strengthened by the robust visual perception of human-designated information, such as traffic signs [33], [34], pedestrians, vehicles, road, as well as other kinds of traffic participants. Benefiting from the progress of saliency computation models, driver attention that directly links the driving task and eye fixation was focused, and had been exploited into the many kinds of applications, such as novelty detection [35] (denoting the irregular observation discrimination to a learned model), important object detection [36]–[38], periphery-fovea driving model designing [8], and so on.

In order to mimic the real driver attention mechanism for large-scale and diverse traffic scenarios, Palazzi *et al.* launched the DR(eye)VE project [13] that exploited the driver fixation pattern in an actual car exposed to sunny and unobstructed traffic scene, and on this basis, several models based on deep neural networks (e.g., fully connected network (FCN), multi-branch 3D CNN) [16], [17], [39]–[41] were built for driver attention prediction. However, DR(eye)VE only collected 8 drivers's gazing behavior having the large subjective difference. Beside DR(eye)VE, there were also some attempts [16], whereas the datasets in these attempts were annotated coarsely and cannot reflect the practically dynamic driving behavior.

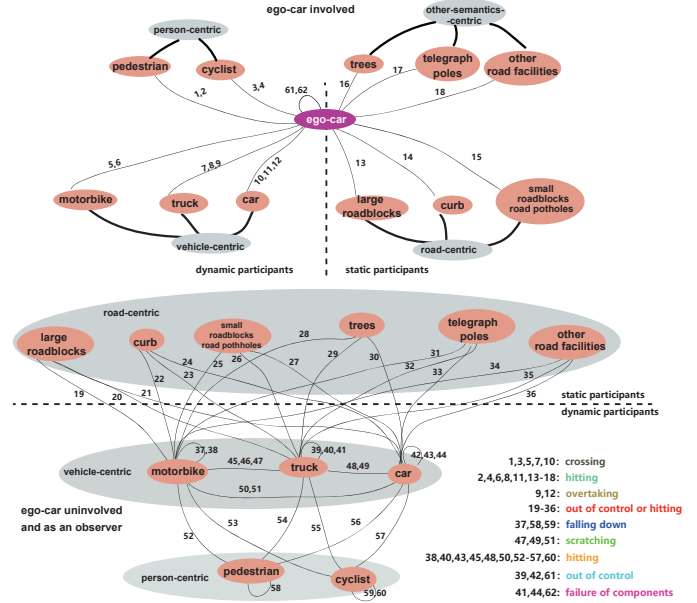


Fig. 2. The ego-car involved and ego-car uninvolved accident category graph in driving scene, where each kind of accident category is explained.

More recently, Berkeley DeepDrive Laboratory constructed a large-scale driver attention dataset in-lab focusing on the critical situations, named as BDDA [14], and built a simple convolutional neural networks (CNN) to predict the driver fixations. BDD-A is the most relative one to our work, whereas it does not consider the dynamic attention process from the critical situations to actual accidents. In the meantime, they did not categorize the braking events into sub-classes, which may be more useful for avoiding certain accident. In this paper, we provide a larger and more diverse driver attention prediction benchmark than ever before, and propose a novel driver attention prediction model in accidental scenarios considering the semantic and vision variations.

III. DADA-2000 DATASET

Because of the rather rarity of the accidental scenarios, we searched almost all the public datasets and the mainstream video websites, such as Youtube, Youku, Bilibili, iQiyi, Tencent, etc., and obtained about 3 million frames of videos. However, these videos have many useless typing masks. Therefore, we have conducted a laborious work for washing them, and obtained 658,476 available frames contained in 2000 videos with the resolution of 1584×660 (=6.1 hours with 30 fps, over than DR(eye)VE [13]). Different from the existing works with a strict trimming of frames [14], [42] (such as the last ten frames as the accident interval) for accident annotation, we advocate a free presentation without any trimming work. In this way, the attention collection maybe more natural.

A. Accident Annotation

1) *Accident Categories:* Since this work focuses on the accidental scenarios, we further divide these videos into 54 kinds of categories based on the participants of accidents (pedestrian, vehicle, cyclist, motorbike, truck, bus, and other

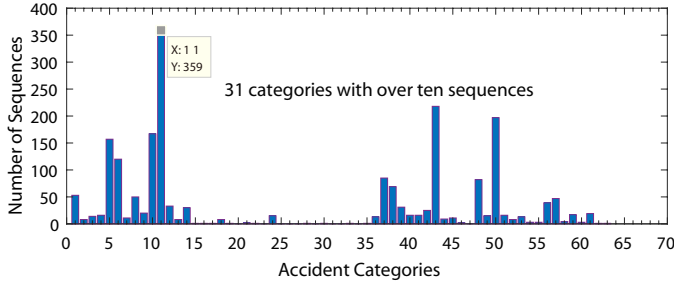


Fig. 3. Video amount statistics w.r.t. accident categories.

static obstacles, etc.), where the illustration of the accident categories can be seen in Fig. 2. Among them, these 54 categories can be classified into two large sets, ego-car involved and ego-car uninvolved. Specifically, the amount distribution of accident categories in our benchmark is illustrated in Fig. 3, respectively. Because the accidents in real world are rather diverse, we have considered 62 categories of the accident situations as complete as possible in practical driving scene. From this distribution, the *ego-car hitting car* takes the largest proportion.

TABLE I

THE ATTRIBUTES, W.R.T., LIGHT CONDITION AND WEATHER CONDITION.

DADA-2000	Light condition		Weather condition		
	daytime	nighttime	sunny	rainy	snowy
#videos	1800	200	1860	130	10

TABLE II

THE ATTRIBUTES, W.R.T., SCENE OCCASION.

DADA-2000	Scene occasion			
	highway	urban	rural	tunnel
#videos	1420	380	180	20

2) *Scene Diversity*: In addition, we also present the scene diversity of DADA-2000 by Table. I and Table. II. From these tables, we can see that because of the more frequent and diverse transit trip in daytime and urban scene than nighttime and other occasions, the highest occurrence rate of accidents is shown.

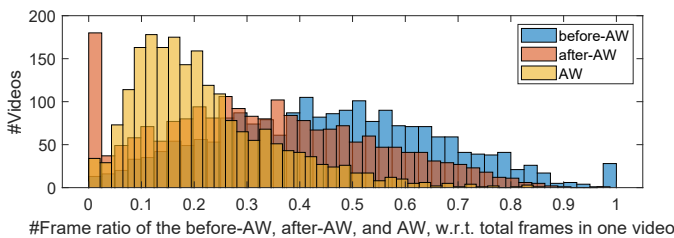


Fig. 4. The frame interval distribution of before-AW, after-AW, and AW in the videos.

3) *Temporal Statistics*: In DADA-2000, we annotated the spatial crash-objects, temporal window of the occurrence of accidents, and collected the attention map for each video

TABLE III

THE TEMPORAL FRAME STATISTICS OF THE NUMBER OF FRAMES AND AVERAGE FRAMES OF ALL VIDEOS, BEFORE-AW, AW, AND AFTER-AW, WHERE AW REPRESENTS THE ACCIDENT WINDOW.

Statistics	total	before-AW	AW	after-AW
#total frames	658,476	315,154	131,679	211,643
#average frames	330	157	66	106
#percentage (%)	100	47.6	20.0	32.1

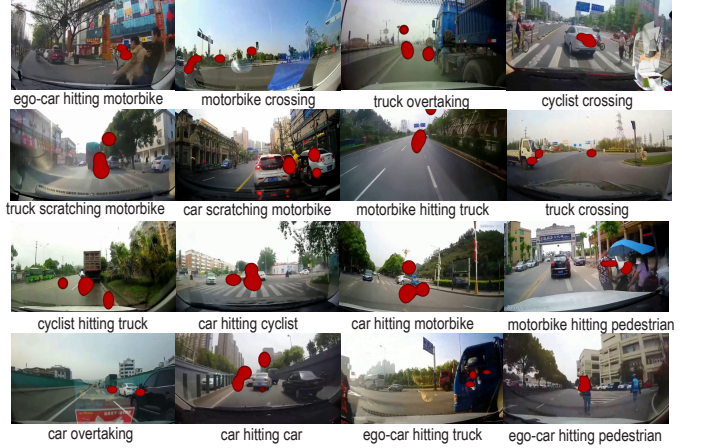


Fig. 5. Frame examples with ground-truth FTA-Fixations for 16 kinds of accidental scenarios. The larger red-spot in FTA-Fixations means longer focusing time.

frame. For a video sequence, we partitioned it into three main clips: the frame interval before the accident window (before-AW), accident window (AW) and the frame interval after the AW (after-AW). For AW determining, if half part of the object that will occur accident (we define it as crash-object in this paper) appears in the view plane, we set the frame as the starting point, and set the frame as the ending point if the scene returns a normal moving condition.

The frame interval distributions of before-AW, AW, and after-AW are presented in Fig. 4, and the averages of them are listed in Table. III. From these statistics, we find that before-AW contains about 5 seconds of time (30fps) in average and after-AW takes about 3.5 seconds of time. AW takes a percent of 20% in each video averagely. Therefore, the frames of abnormal driving are rather fewer than the ones in normal driving.

We also compare our DADA-2000 with the state-of-the-art datasets concentrating on the driving accident detection or prediction in Table. IV. From Table. IV, we can observe that our DADA-2000 has more diverse scenarios and is more complex for driving accident analysis. This will provide a new platform for driving accident detection or prediction problem.

B. Attention Collection

1) *Protocols*: Because of the rarity of the accident in practical driving, in our attention collection protocol, we employed 20 volunteers with at least 3 years of driving experience. The eye-tracking movement data were recorded in a laboratory by a Senso Motoric Instruments (SMI) RED250 desktop-mounted infrared eye tracker with 250 Hz. In order to approach the real

TABLE IV
ATTRIBUTE COMPARISON OF DIFFERENT DRIVING ACCIDENT DATASETS.

Dataset	videos	accidents	all frames	typical participants	annotation type
Street Accidents (SA) [42]	994	165	99,400	car, truck, bike	temporal
A3D** [43]	1500	1500	208,166	car, truck, bike, pedestrian, animal	temporal
DADA-2000	2000	2000	658,476	car, truck, bike, pedestrian, animal, motorbike, static obstacles	spatial and temporal

TABLE V
THE ATTRIBUTE COMPARISON OF DIFFERENT DRIVER ATTENTION DATASETS

dataset	rides	durations(hours)	drivers	gaze providers	event	gaze patterns for each frame
DR(eye)VE [13]	74	6	8	8	464 braking events	attention map of single person
BDD-A [14]	1232	3.5	1232	45	1427 braking events	average attention map of multiple observers
DADA-2000	2000	6.1	2000	20	2000 accidents (54 categories)	raw attention maps of multiple observers

driving scene, we weaken the lighting of the lab to reduce the impact of surroundings, by which only the computer screen is focused. In addition, we asked the volunteers to be relaxed and imagine that they were driving real cars. For avoiding the fatigue, we let each volunteer watch 40 clips on a 21' screen each time which are combined as a single long sequence with about 7 minutes. Each clip was viewed at least by 5 observers. It is worthy noting that, we ensure that the 40 video sequences belonging to the same accident category as much as possible, so as to prevent chaotic attention.

2) *Attention Type*: For the attention map of a frame, there was a parameter determining the time window which aggregated the attentions within it to generate an attention map for a frame (1 second was utilized in DR(eye)VE). This setting can reserve the dynamic attention process in a small temporal window, but not be constructive to the crash-object localization. Therefore, in this work, we recorded the fixation without temporal aggregation, but differently we recorded the focusing time of each fixation in each frame to represent the temporal attention information (we denote this kind of fixation as focusing time allocated fixation, *abbrev.*, FTA-Fixation), as shown in Fig. 5 demonstrating some frameshots with FTA-Fixations of typical accidental scenarios. Notably, different from the works [13], [14], we did not average the attention fixations of observers and maintain them in the same frame because of their subjectivity. The frame rate of the attention maps were all recorded in 30fps, and we captured the attention data for all of the frames in our DADA-2000. The attribute comparison with other state-of-the-art driver attention datasets is presented in Table. V. From this comparison, our DADA-2000 is more diverse, and contributes a new benchmark for driver attention prediction, and other benchmarks concentrating on driving scene can be seen in [44].

3) *Capacity of Human Attention for Predicting Accidents*: In this work, we analyzed the average delayed frames (ADF) ahead or behind the starting boundary of accident window where the crash-object were noticed for the first time by human eyes for 26 kinds of accidents observed crash-objects³. This analysis gives a general conclusion for which kind of accident can be predicted ahead or behind of its occurrence by

³In DADA-2000 benchmark, we detected the objects in each frame and the crash-object may be found by the detector or not found by the detector because of the complex scenes. We take the video sequences in which the crash objects were detected in this statistics.

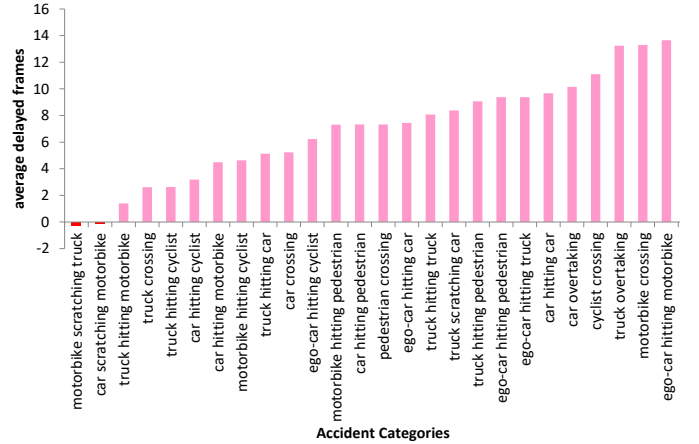


Fig. 6. The statistics of # average delayed frames (ADF) with an ascending order, w.r.t., 26 kinds of accidental scenarios.

human eyes. For this analysis, we firstly detected the objects in each frame by the popular YOLO-V3 detector [45], and determined the crash-object in each frame. Then we checked whether the peak location of the attention map hit the crash-object (1-hit, and 0 for vice versa). Through extensive statistics for all the sequences of the 26 kinds of accidental scenarios observed crash-objects, we obtained the average ADF value for each kind of accident. The results are shown in Fig. 6 with an ascending order of ADF values. From this figure, we can observe that in our benchmark human eyes show the worst expression for *ego-car hitting motorbike* category, and demonstrate perfect focusing performance on *motorbike scratching truck* even with a negative ADF. Broadly speaking, human eyes are often with a delayed aware of crash-objects, while the largest ADF is 13 frames only taking about a half of second (30fps in DADA-2000). Therefore, driver attention is a promising cue for driving accident prediction.

C. Training/testing Splits

Because there are over 650,000 frames in DADA-2000, it is very huge and not easy to train. Therefore, in this work, we selected half of the videos (1000 videos) for training, validation and testing. Notably, we still maintain the same number of the accidents (54 categories), even that some ones only has one sequence. Then, we partitioned the selected

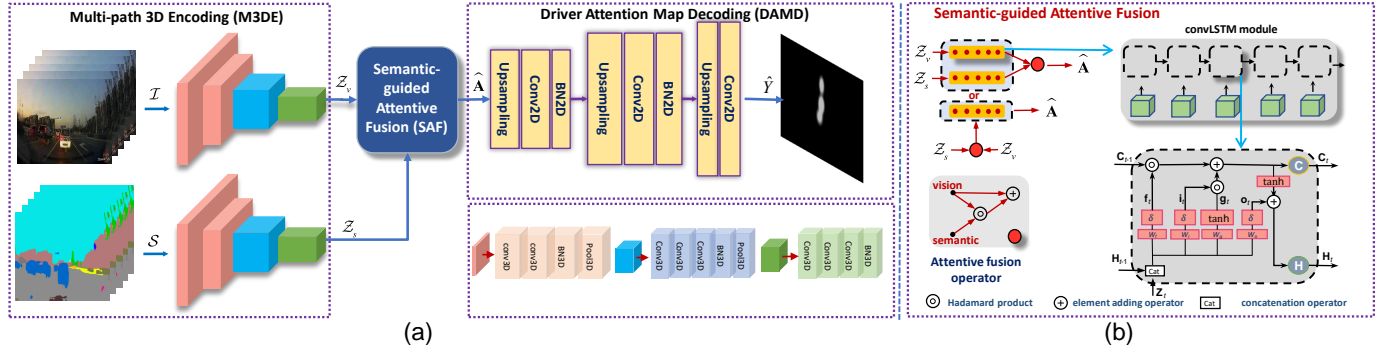


Fig. 7. (a) is the architecture of the proposed approach and (b) illustrates the flowchart of the semantic-guided attentive fusion module. Given a video clip \mathcal{I} , we firstly obtain the semantic images \mathcal{S} by popular semantic segmentation models. Then the vision clip and the semantic clip are fed into the multi-path 3D feature encoding pipeline interleaved many kinds of 3D blocks, interleaved in 3D convolution (conv3D), 3D batch normalization (BN3D), and 3D pooling (Pool3D) blocks, which generates the hidden representations of vision clip (\mathcal{Z}_v) and semantic clip (\mathcal{Z}_s), respectively. Furthermore, \mathcal{Z}_s and \mathcal{Z}_s are taken into the input of the semantic-guided attentive fusion module with an enforcement of semantic variation in spatio-temporal attention prediction, and output the hidden driver attention maps $\hat{\mathbf{A}}$, which is then decoded for the final attention map $\hat{\mathbf{Y}}$ of the last frame in the clip with interleaved upsampling, 2D convolution, and batch normalization operations. (This figure should be viewed in color mode.)

videos as the ratio of about 3:1:1 for training, validation and testing, i.e., 598 sequences (with about 214k frames), 198 sequences (about 64k frames), and 222 sequences (with about 70k frames), respectively. If some kinds of accidents have only one video, we take them into the testing part.

IV. OUR APPROACH

The architecture of the our multi-path semantic-guided attentive fusion network (MSAFNet) for driver attention prediction is demonstrated in Fig. 7. Given a video clip with several frames, the architecture predicts the driver attention map of a last frame within the clip. There are three modules in the proposed method: a multi-path 3D encoding (M3DE) architecture, a semantic-guided attentive fusion module (SAF), and a driver attention map decoding module (DAMD). M3DE aims to extract the spatio-temporally hidden representation of vision and semantics within the given video clip, where the semantic images of the clip are obtained by the popular deeplabv3 [46] pre-trained on the renowned semantic segmentation benchmark Cityscapes [47]. SAF learns to transfer the spatio-temporal hidden representations of the vision and semantics of the clip to its last frame, and combines them together with an attentive fusion strategy. One more word, SAF fulfills a casual inference of the hidden representations of the vision and semantic essentially. 3) DAMD generates the final attention map of the last frame in the given clip. In the following subsections, we will elaborate each module in details.

A. The M3DE Architecture

The M3DE architecture aims to extract the spatio-temporal motion nature of the vision and semantics and exploit their hidden representation for dynamic observation of traffic scene. The motivation is that in driving scenarios driving task plays a vital role for the target or routine searching for drivers, and based on the investigation, semantic of the traffic scene is knowledgeable to the driving policy learning, and has been

utilized in many recent driving models [48], [49]. Considering this, we introduce the semantic information of the scene to reflect the driving policy indirectly.

Formally, assume we have the video clip \mathcal{I} , consisting of T frames $\{I_t\}_1^T$. We firstly obtain the semantic images $\{S\}_1^T$ of \mathcal{I} by a popular semantic segmentation approach deeplabv3 [46] pre-trained by the Cityscapes [47]. Then, $\{S\}_1^T$ and $\{I\}_1^T$ are fed into each path of M3DE as input, respectively. Here, a 3D CNN architecture is constructed for encoding the spatial and sequential hidden representation of $\{S\}_1^T$ and $\{I\}_1^T$, respectively, and consists of four integrations of 3D blocks exploiting the spatio-temporal representation in different scales, interleaved by several 3D conv blocks (conv3D), 3D batch normalization block (BN3D) and 3D pooling block (Pool3D), where BN3D is utilized to accelerate the convergence and resist the gradient vanishing.

In our implementation, we resize the input successive frames as the resolution of 256×256 . Differently, we have RGB channels for each original image and one channel for each semantic image. The 3D CNN contains four integrations, with 18 layers of 3D blocks, as shown in Fig. 7. The detailed parameter configuration of each layer is demonstrated in Fig. 8, where the kernel size of conv3D is $3 \times 3 \times 3$. Notably, each conv3D block followed a rectified linear unit, i.e., *Relu*. After passing M3DE architecture, we obtain the spatio-temporally hidden representation $\mathcal{Z}_v = \{\mathbf{Z}_t^v\}_{t=1}^T$ and $\mathcal{Z}_s = \{\mathbf{Z}_t^s\}_{t=1}^T$ for the vision and semantics paths, and then they are fed into the following SAF module. Notably, $\mathcal{Z}_s, \mathcal{Z}_v \in \mathbb{R}^{T \times 512 \times 32 \times 32}$ are 4D tensors owning 512 feature maps with 32×32 resolution for T frames.

B. SAF Module

Fig. 7(b) demonstrates the flowchart of the SAF module. With the hidden representation \mathcal{Z}_v and \mathcal{Z}_s of original RGB images and semantic images, we insightfully design a fusion strategy to explore the complementary characteristics of them. In this work, we adopt the conv-LSTM to learn and transfer

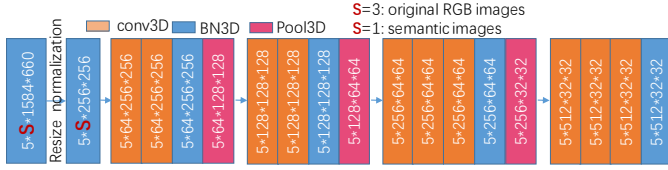


Fig. 8. The parameter configuration of M3DE architecture.

the spatio-temporally hidden representations of vision and semantic in successive frames within the input clip to its last frame. In other words, conv-LSTM here acts as a messenger to transfer the spatio-temporal dynamics within the clip to the last frame. Then, we treat the transitioned hidden representation of the last frame in semantic path as an attention operator, and design a semantic-guided attentive fusion (SAF) module to enforce the spatio-temporal semantic clue attentively to the vision path. Denote the output of SAF as an hidden driver attention representation $\hat{\mathbf{A}}$. Considering the fusion stage (later fusion or early fusion), we formulate SAF as two forms:

$$\begin{aligned}\hat{\mathbf{A}} &= \mathcal{G}(f(\mathbf{Z}_v, \mathbf{W}_v), f(\mathbf{Z}_s, \mathbf{W}_s)), \text{ or} \\ \hat{\mathbf{A}} &= f(\mathcal{G}(\mathbf{Z}_v, \mathbf{Z}_s), \mathbf{W}),\end{aligned}\quad (1)$$

where \mathcal{G} denotes the attentive fusion operator, $f(\cdot, \cdot)$ specifies the conv-LSTM module with the parameters \mathbf{W}_v , \mathbf{W}_s or \mathbf{W} for vision path, semantic path or the fused path, respectively.

1) *Transition of Spatio-temporal Dynamics*: Conv-LSTM extends the LSTM by preserving the spatial details in predicting when learning the temporal dynamics, which contains the memory cell \mathbf{C}_t , hidden states \mathbf{H}_t of time t to control the memory update and the output of \mathbf{H}_t , and transfer the dynamics in temporal steps when inputting \mathbf{Z}_t (Here, we omit the distinction for vision path and semantic path), respectively. Precisely, convLSTM is computed as follows:

$$\begin{aligned}\mathbf{i}_t &= \sigma(W_{zi} * \mathbf{Z}_t + b_{zi} + W_{hi} * \mathbf{H}_{(t-1)} + b_{hi}) \\ \mathbf{f}_t &= \sigma(W_{zf} * \mathbf{Z}_t + b_{zf} + W_{hf} * \mathbf{H}_{(t-1)} + b_{hf}) \\ \mathbf{g}_t &= \tanh(W_{zg} * \mathbf{Z}_t + b_{zg} + W_{hg} * \mathbf{H}_{(t-1)} + b_{hg}) \\ \mathbf{o}_t &= \sigma(W_{zo} * \mathbf{Z}_t + b_{zo} + W_{ho} * \mathbf{H}_{(t-1)} + b_{ho}) \\ \mathbf{C}_t &= \mathbf{f}_t \circ \mathbf{C}_{(t-1)} + \mathbf{i}_t \circ \mathbf{g}_t \\ \mathbf{H}_t &= \mathbf{o}_t \circ \tanh(\mathbf{C}_t)\end{aligned}\quad (2)$$

where σ and \tanh are the activation functions of logistic sigmoid and hyperbolic tangent, respectively. “ $*$ ” and “ \circ ” denote the convolution operator and Hadamard product, and $\mathbf{i}_t, \mathbf{f}_t, \mathbf{o}_t$ are the convolution gates controlling the input, forget and output, respectively. Notably, \mathbf{H}_0 and \mathbf{C}_0 are initialized as 3D tensors with zero elements owning the same dimension to the input $\mathbf{Z} \in \mathbb{R}^{512 \times 32 \times 32}$.

2) *Attentive Fusion*: Since this work aims to fulfill an attentive fusion, we enforce the hidden representations $\{\mathbf{Z}_t^s\}_{t=1}^T$ of T frames in semantic path or the hidden state \mathbf{H}_T^s as an attention tensor to select the feature representation in $\{\mathbf{Z}_t^v\}_{t=1}^T$ or \mathbf{H}_T^v for early fusion or later fusion, respectively. Inspired by the recent attention mechanism [15], [24], [31], we introduce

a residual connection to maintain the original information in vision path after fusion. Therefore, we define $\hat{\mathbf{A}}$ as:

$$\begin{aligned}\hat{\mathbf{A}} &= \mathcal{G}(\mathbf{H}_T^v, \mathbf{H}_T^s) = \mathbf{H}_T^v \circ (1 + \mathbf{H}_T^s), \text{ or} \\ \hat{\mathbf{A}} &= f(\mathcal{G}(\mathbf{Z}_v, \mathbf{Z}_s), \mathbf{W}) = f(\mathbf{Z}_v \circ (1 + \mathbf{Z}_s), \mathbf{W}),\end{aligned}\quad (3)$$

where $f(\cdot, \cdot)$ is the conv-LSTM module. Fig. 7 (b) demonstrates the SAF module. By this kind of semantic-guided attentive fusion, we fulfill a feature representation selection while maintained the original information of vision path.

C. DAMD module

After obtaining the hidden driver attention representation $\hat{\mathbf{A}} \in \mathbb{R}^{256 \times 32 \times 32}$ with 256 channels of 32×32 resolution, it is fed into the driver attention map decoding module (DAMD) to generate a driver attention map \hat{Y} of the last frame in each clip, with the same size to the input frames, where 8 layers interleaved several 2D convolution, 2D batch normalization (BN2D), and upsampling layers. Specifically, DAMD module is implemented as upsampling($\times 2$) \rightarrow conv(3×3 , 128) \rightarrow BN2D \rightarrow upsampling($\times 2$) \rightarrow conv(3×3 , 64) \rightarrow BN2D \rightarrow upsampling($\times 2$) \rightarrow conv(3×3 , 1), where the conv is denoted as conv(kernel, channel). Note that, each conv layer follows a *Relu* function, and the last layer in our network is a *Sigmoid* function to limit the output value of driver attention map to $[0, 1]$.

D. Learning

In this work, we have the ground-truth driver attention map Y , the predicted attention map \hat{Y} , the learning is to make the massive predicted \hat{Y} approximate to Y . Different from the previous video attention prediction models which introduced the fixation point (reflecting the location points noticed by human eyes) and blurred attention maps obtained by a smoothing around the fixation points with a Gaussian kernel as the ground-truth, we take the FTA-Fixation (defined in Sec. III-B) automatically recorded by the eye-tracker as the ground-truth because the more information of fixation and focusing time. Because the resolution of Y and \hat{Y} is the same, which can be directly utilized to the loss computation.

Assume we have M clips in each training batch, where each clip, as aforementioned, owns T consecutive frames. Each clip outputs one driver attention map. Formally, our loss function is defined as:

$$\mathcal{L}(Y, \hat{Y}) = \mathcal{L}_{KL}(Y, \hat{Y}) + \mathcal{L}_{CC}(Y, \hat{Y}), \quad (4)$$

where \mathcal{L}_{KL} is the Kullback-Leibler (KL) divergence evaluating the distribution distance of two maps, successfully used in previous saliency detection methods, and \mathcal{L}_{CC} represents the Linear Correlation Coefficient (CC) widely adopted in the saliency evaluation metrics, measuring the linear relationship between \mathcal{Y} and $\hat{\mathcal{Y}}$. \mathcal{L}_{KL} and \mathcal{L}_{CC} are defined as:

$$\begin{aligned}\mathcal{L}_{KL}(Y, \hat{Y}) &= \sum_i Y(i) \log \left(\epsilon + \frac{Y(i)}{\epsilon + \hat{Y}(i)} \right), \\ \mathcal{L}_{CC}(Y, \hat{Y}) &= -\frac{\text{cov}(Y, \hat{Y})}{\rho(Y)\rho(\hat{Y})},\end{aligned}\quad (5)$$

where $cov(Y, \hat{Y})$ is the covariance of Y and \hat{Y} , $\rho(\cdot)$ refers to standard deviation, the summation index i spans across image pixels and ϵ is a small constant that ensures numerical stability. Because Linear Correlation Coefficient prefers a large value for similar two maps, the \mathcal{L}_{CC} computes its negative value.

In our implementation, each video training batch has 12 clips randomly selected from the training set, and each clip contains 5 successive frames. More detailed implementation can be seen from Sec. V.

V. EXPERIMENTS

A. Implementation Details

As aforementioned, there are huge amount of frames in our DADA dataset. We choose half of them (1000 videos) as the evaluation dataset, and partitioned the training, validation, and testing as a ratio of 3:1:1 with 598 sequences ($\sim 214k$ frames), 198 sequences ($\sim 64k$ frames), and 222 sequences ($\sim 70k$ frames), respectively. In our experiments, we utilized the training set and the testing set for performance evaluation. During training, we adopted the Adam optimizer with the learning rate of 0.0001, $\beta_1=0.9$, $\beta_2=0.999$, and $e = 10^{-8}$. The whole model is trained in an end-to-end manner and trained for 3 epochs. The entire training procedure takes about 27 hours using two NVIDIA RTX2080Ti*GPUs with 22GB RAM.

B. Evaluation Protocols

Following the existing attention prediction works [15], [24], [31], seven quantitative metrics are utilized: Kullback-Leibler divergence (KLdiv), Normalized Scanpath Saliency (NSS), Similarity Metric (SIM), Linear Correlation Coefficient (CC), AUC-Judd (AUC-J), and shuffled AUC (AUC-S). The physical meaning of these metrics are as follows.

KLdiv measures the information loss of the probability distribution of predicted maps to the ones of the ground-truth, and the smaller value prefers a less information loss.

NSS computes the average value of the positive positions in predicted attention map, which measures the hitting rank to the ground-truth fixations, and higher value is better. Actually, with the SMI-250 eye-tracker, FTA-Fixations are obtained by enlarging the fixation point with a radius whole value represents the focusing time. Therefore, in order to make the AUC-X computable, we selected the locations with peak value, and obtained 5-10 fixation points in each frame. It agrees the attention collection protocol with at least five observers seen each video.

SIM concerns the interaction of the predicted attention map and the ground-truth, which pursues a probability distribution with same shape, and larger value means the predicted attention map cover the similar regions to the ground-truth.

CC calculates the linear relationship of the random variables in two distributions, and similarly the higher value shows a better matching of the distributions.

AUC-X computes the area under the curve with different criteria for evaluation, with respect to different binary segments of predicted attention map approximating the fixations with distinct levels ranging from [0,1].

TABLE VI

THE PERFORMANCE COMPARISON OF THE ABLATION STUDY. THE SYMBOL \uparrow PREFERENCES A LARGER VALUE AND \downarrow EXPECTS A SMALLER VALUE. THE BEST ONE ARE MARKED BY THE **BOLD** FONT.

Baselines	SIM \uparrow	CC \uparrow	KLdiv \downarrow	NSS \uparrow	Auc-S \uparrow	Auc-J \uparrow
ours/S	0.2027	0.3377	2.984	2.2575	0.6383	0.9234
ours-S-EF	0.2062	0.3324	3.3072	2.2049	0.6393	0.9227
ours-S-LF	0.2058	0.3420	2.8940	2.2664	0.6386	0.9255

TABLE VII

THE PERFORMANCE COMPARISON BETWEEN THE PROPOSED METHOD AND THE SEVEN STATE-OF-THE-ART APPROACHES. THE SYMBOL \uparrow PREFERENCES A LARGER VALUE AND \downarrow EXPECTS A SMALLER VALUE. THE BEST ONE ARE MARKED BY THE **BOLD** FONT.

Methods	SIM \uparrow	CC \uparrow	KLdiv \downarrow	NSS \uparrow	Auc-S \uparrow	Auc-J \uparrow
SALICON [50]	0.183	0.302	3.589	1.989	0.634	0.908
SalGAN [51]	0.192	0.311	4.507	2.063	0.618	0.906
BDDA [14]	0.151	0.258	3.905	1.702	0.623	0.884
DR(eye)VE [13]	0.077	0.089	8.050	0.605	0.516	0.805
MLNet [52]	0.058	0.104	4.847	0.673	0.582	0.788
TwoStream [53]	0.082	0.177	3.298	1.204	0.544	0.861
ACLNet [15]	0.214	0.273	7.614	1.818	0.595	0.883
ours-S-LF	0.206	0.342	2.894	2.266	0.639	0.926

For validating the performance, this work first carries out the ablation study for evaluating the core components of the whole model, and then gives the evaluation comparison between the proposed model with the state-of-the-arts. Moreover, we present more analysis on the driver attention prediction ability for different accident attributes, capacity comparison of humans and our model for early accident prediction, and also investigate the object detection in finding crash objects.

C. Ablation Study

In this work, taking the vision path with spatio-temporal variation representation as the fundamental basis, we 1) enforced spatio-temporal semantic variation on this basis, and 2) designed the attentive fusion strategy. Therefore, we have three kinds of baselines to check the influence of these components. They are “ours-w/o-semantic (**ours/S**)”, “ours-with-semantic early fusion (**ours-S-EF**)”, and “ours-with-semantic later fusion (**ours-S-LF**)”, denoting the model with only vision path, the full model with early fusion, and the full model with later fusion, respectively.

The quantitative results are listed in Table. VI. From the results, we can see that the full model considered the spatio-temporal semantic variation has been improved but with a tiny difference, and the later fusion is better than the early fusion. The underlying reason may be that although the semantic information can provide a task-related information for this work, the segmentation approach may be powerless for the challenging situations, such as the frequent heavy rain and low illumination condition, and could introduce noise to the vision path. Therefore, the early fusion has week performance. However, as a framework for better generalization for the driver attention prediction, we provide the full model with later fusion for this work and may be improved with better semantic segmentation methods in future.

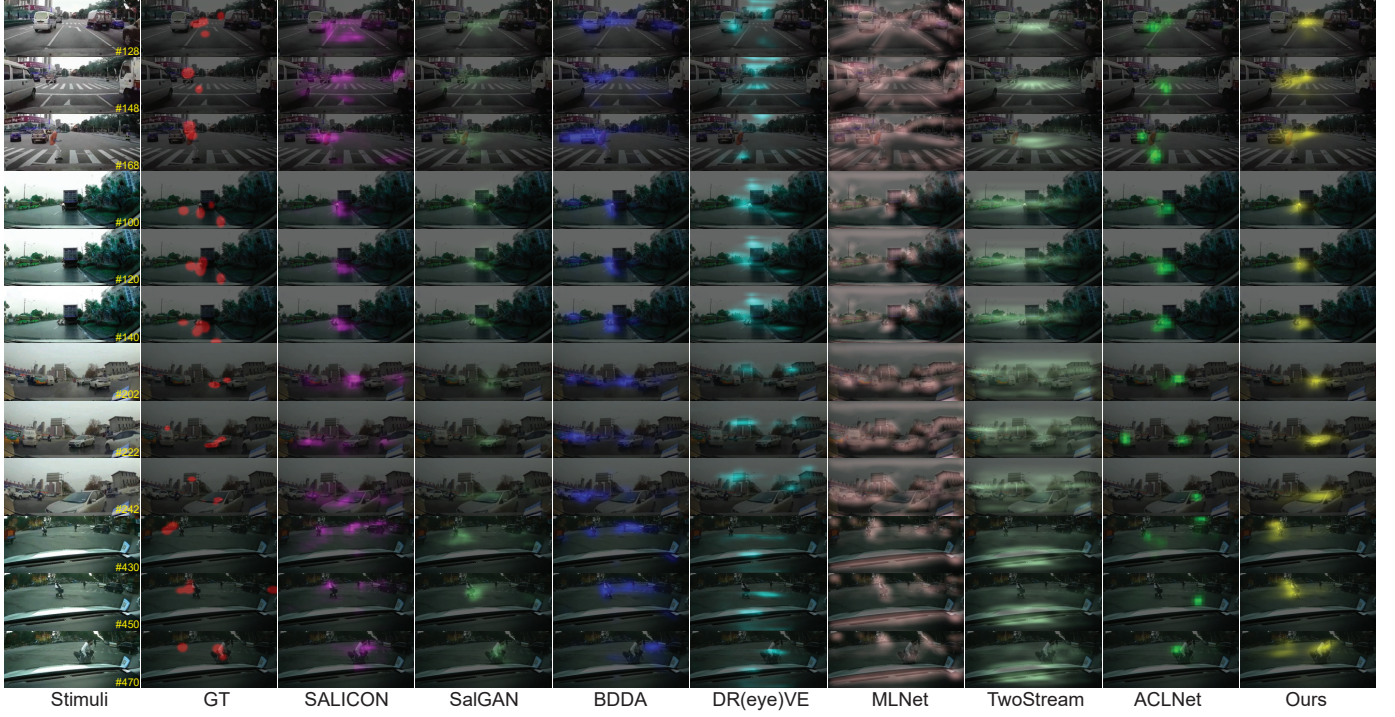


Fig. 9. The visualized snapshots demonstrating the attention prediction results by SALICON [50], SalGAN [51], BDDA [14], DR(eye)VE [13], BDDA [14], DR(eye)VE [13], MLNet [52], TwoStream [53], ACLNet [15] and our model from left to right columns, respectively. GT means the ground-truth of FTA-Fixations. (This figure should be viewed in color mode.)

D. Comparison with State-of-the-arts

In order to verify the superiority of the proposed method, we introduce seven attention prediction methods representing the state-of-the-arts, consisting of five dynamic ones, i.e., BDDA [14], DR(eye)VE [13], TwoStream [53], MLNet [52], ACLNet [15], and two static ones, i.e., SALICON [50] and SalGAN [51]. Among them, BDDA and DR(eye)VE are two classic ones concentrating the driver attention prediction in critical situations and normal scenarios, respectively, and other ones focused on the general video attention prediction problem. The codes of the competing approaches are downloaded from their official website and re-trained by our DADA benchmark with the same configuration stated in their works. The original configuration of DR(eye)VE had three kinds of inputs, the RGB channel, the semantic channel, and the optical flow channel. In this work, we take the RGB and semantic channel the same as our work to re-train their model.

Table. VII presents the quantitative results of the proposed method and other state-of-the-arts. From these results, our full model with later fusion (ours-S-LF) outperforms others significantly. Interestingly, we find that except from our model, most of the metrics of static attention methods show higher values than the dynamic ones. The underlying reason may be two fold: 1) static methods do not consider the complex motion or variation information in prediction, which could reduce the influence of the historical dynamics of scene that may be considered inadequately; 2) the behind mechanisms of dynamic driver attention allocation in challenging situations is complex and still unclear, which can enforce the difficulty to the spatio-temporal attention prediction model. Especially

for the complex motion condition and various environment situations, the other dynamic objects in the background can easily disturb the prediction, as shown in by the results of TwoStream [53] in Table. VII.

In the dynamic attention prediction approaches, ACLNet generates the best SIM value while other metric values are not good enough. That is because the temporal consistency of our benchmark is not strong and with many variations, commonly reflected as the sudden fixation change when noticed the crash-object. On the contrary, we have a smaller frame duration in each input clip (5 frames) than ACNet (20 frames) to adapt this sudden change, and introduce the semantic variation to enforce the attention allocation. DR(eye)VE designed a shallow multi-branch 3D encoding module to represent the spatio-temporal variation (16 frames as input), which may be not adequate for the accidental scenarios with frequent motion and scene change. Therefore, the poor performance is generated. However, because of the large weight assignment for the critical frames, BDDA demonstrates a stable and good performance except from our method.

For quantitative evaluation, we demonstrate some frame snapshots of different approaches in Fig. 9. From this figure, we can see that other methods are disturbed by other dynamic objects in background more or less, and the crossing person (in the first sequence in Fig. 9) has been noticed early by our model and a compact attention map is generated to the hit motorbike (in the second sequence in Fig. 9). Interestingly, an attention transition from the road vanishing point to the crossing person appeared in our model. The crash-object are noticed by the static attention prediction methods (SalGAN

TABLE VIII

THE PERFORMANCE OF FIVE DYNAMIC ATTENTION PREDICTION METHODS ON THREE KINDS OF TYPICAL BEHAVIORS IN ACCIDENTAL SCENARIOS, I.E., THE CROSSING, HITTING AND OUT OF CONTROL OF EGO VEHICLE AND OTHER CRASH VEHICLES. THE VALUES IN THIS TABLE ARE THE AVERAGE OF ALL RELATED VIDEOS IN THE TESTING SET. THE NUMBER IN THE BRACKET IS THE NUMBER OF THE VIDEOS IN EACH BEHAVIOR TYPE. THE BEST VALUE OF EACH METHOD WITH RESPECT EACH METRIC IN DIFFERENT BEHAVIOR TYPE ARE MARKED IN **BOLD FONT**.

behavior types in accidents	crossing (42)				hitting (94)				out of control (19)			
methods/metrics	NSS↑	SIM↑	CC↑	Kldiv↓	NSS↑	SIM↑	CC↑	Kldiv↓	NSS↑	SIM↑	CC↑	Kldiv↓
BDDA [14]	1.6463	0.1117	0.2183	3.7907	1.6887	0.1440	0.2484	3.9379	1.5750	0.1977	0.2964	4.4853
DR(eye)VE [13]	0.6039	0.0603	0.0760	9.1440	0.7083	0.0792	0.0979	6.9220	0.4121	0.0760	0.0726	10.4259
mlNet [52]	0.6226	0.0414	0.0812	5.0336	0.6507	0.0546	0.1010	4.9253	0.6443	0.0692	0.1106	5.0436
TwoStream [53]	1.2138	0.0630	0.1615	3.4739	1.2901	0.0804	0.1825	3.1544	0.9800	0.0969	0.1799	3.4453
ACNet [15]	1.8104	0.1701	0.2360	6.8620	1.9173	0.2179	0.2813	7.2759	1.6377	0.2483	0.2972	8.5894
ours-S-EF	2.3764	0.1712	0.3128	3.1990	2.2596	0.2027	0.3337	3.2623	2.1314	0.2634	0.3857	3.1726
ours-S-LF	2.3535	0.1628	0.3128	3.0087	2.3162	0.2017	0.3412	2.8056	2.2441	0.2734	0.4066	2.7019

and SALICON) which focus on the frame-by-frame prediction without the temporal dynamic consideration. On the contrary, the dynamic models often drift attention to other irrelevant objects. Especially, MLNET and TwoStream show indiscriminate focusing to dynamic objects in the background.

E. Further Analysis

1) *Comparison w.r.t., Behavior Type in Accidental Scenarios*: In this work, we also evaluate the performance of dynamic attention prediction methods on different type of behaviors in accidental scenarios. Specifically, we partitioned the video sequences in the testing set into three sets: “crossing”, “hitting” and “out of control”, and listed the average results with respect to each behavior type in Table. VIII. The results show that our model is the best over different behavior types in accidental scenarios. Except from our model, other approaches show the best NSS value and have the least information loss (lower KLdiv) in “hitting” behavior. As for the crossing behavior, only our model shows a better results than other two behavior types, which indicates that our model can find the crossing object for the best. As for the out of control, most of the methods generate better CC and SIM values.

In order to show the behind reason of these phenomena, we demonstrate the average attention map with respect to different behavior types in Fig. 10. From these maps, we can observe that the fixations tend to the middle of the field of vision (FOV) (Fig. 10(b)) for the hitting scenarios satisfying the center-surround bias assumption better than the ones of “crossing” and “out of control”. However, crossing behavior is dispersive, and has a longer tail to the sides of FOV (Fig. 10(a)). For the “out of control” category, because there is no clear crash-object in these scenarios, the attention may show a frequent variation due to dramatic camera view change, and exhibits a wide range of distribution of fixations, shown by Fig. 10(c). Consequently, the largest CC and SIM are obtained by most of methods on the “out of control” scenarios. Therefore, although the crash-object locations demonstrate a convergence of FOV, different accident categories with differing participants have diverse occurrence patterns of locations.

2) *Humans vs Our Model for Early Accident Prediction*: Beside the performance comparison on different behaviors in accidental scenarios, we also analysis the capability for early accident prediction by humans and our model. To make a comparable analysis, we computed the average delayed

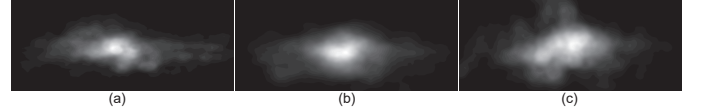


Fig. 10. The average attention map of (a) “crossing” behavior, (b) “hitting” behavior and (c) “out of control” in accidental scenarios in the testing set of DADA-2000.

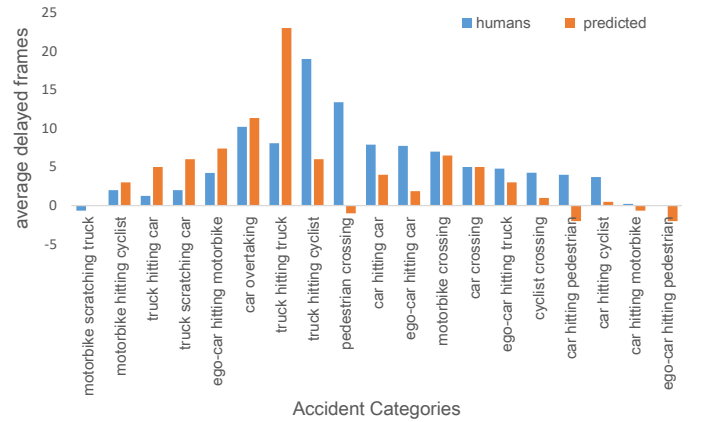


Fig. 11. The statistics of # average delayed frames (ADF), w.r.t., 19 kinds of accidental scenarios of humans and our model.

frames (ADF) of humans and our model in the testing set of DADA-2000, and demonstrate the results in Fig. 11. It is worthy noting that we have obtained effective results for 19 kinds of accidental scenarios because the object detection method cannot work for some videos with complex scene. From this figure, we observe that our model has two-side role for different accidental scenarios, i.e, outperforming humans in some ones and worse than humans for some other ones. Beside the “ego-car hitting motorbike”, the prediction of our model on ego-car involved situations (e.g., ego-car hitting car/truck/pedestrian) are improved and outperforms humans to a large extent, and even achieves an advanced prediction for pedestrians. This is promising for ego-car centered safe driving. Additionally, the crossing behaviors of pedestrian, motorbike and cyclist are predicted better than humans, even with an advanced prediction for pedestrian crossing (with a negative ADF). This observation also confirms a positive role of our model for predicting the crossing behavior to avoid accidents.



Fig. 12. Some frames demonstrating the object detection results and the attention prediction results.



Fig. 13. Some failure situations where the driver attention prediction results do not cover the crash-object. The crash object are marked by the red bounding boxes.

3) Object Detection vs Our Model for Finding Crash Objects: Although we made the statistics for the sensitivity of humans and our model for early accident prediction, the computation of average delayed frames (ADF) depends on the object detection results. However, in some situations with challenging illumination and background, the crash object cannot be detected robustly but noticed by our model, as shown by the results on the frames with strong or dark light condition in Fig. 12. These results indicate that the proposed model can adapt to the accidental scenarios better with the learned knowledge from human focusing experience. Certainly, there are also many failures, as shown in Fig. 13 due to the rather difficult environments being indistinguishable by human beings.

VI. CONCLUSION AND DISCUSSIONS

In this work, we investigated the problem of driver attention prediction, and extended previous works concentrating on the normal and critical situations into the accidental scenarios. Novelty, we constructed a diverse and challenging benchmark with 2000 video sequences (named as DADA-2000 with over 650,000 frames) containing the normal, critical and accidental situations together in each video sequence. In addition, we proposed a multi-path semantic-guided attentive fusion network (MSAFNet) to learn and transfer the spatio-temporal vision and semantic variation within the video clip to the frame to be examined for driver attention prediction by conv-

LSTM module, and fulfilled an attentive fusion to enforce the spatio-temporal semantic clue attentively to the vision path. Thorough extensive analysis for the benchmark and comparison experiments with 7 state-of-the-art methods, and superior performance of MSAFNet is obtained. Notably, the proposed model can notice the crash-object earlier than the human beings in some typically accidental scenarios, such as the scenarios with crossing behavior and ego-car involved hitting behavior. Through the efforts of this work, we also open the most important discussion here.

Can driver attention be feasible for driving accident prediction? Whatever we have done, the ultimate goal is to predict the accident early to fulfill a safe driving. Based on the results and analysis in this work, we find human-eye focusing experience is manifestly useful for the driving accident prediction in some scenarios, such as the crossing behavior and the ego-car centered hitting behavior. Certainly, the human attention shows a delayed observation for the crash object, while we can design some insightful models to not only consider the driver attention, but also introduce some other informative clues in driving scene.

REFERENCES

- [1] P. Gershon, K. R. Sita, C. Zhu, J. P. Ehsani, S. G. Klauer, T. A. Dingus, and B. G. Simons-Morton, "Distracted driving, visual inattention, and crash risk among teenage drivers," *American Journal of Preventive Medicine*, vol. 56, no. 4, pp. 494–500, 2019.
- [2] M. L. Cunningham and M. A. Regan, "Driver distraction and inattention," in *Safe Mobility: Challenges, Methodology and Solutions*. Emerald Publishing Limited, 2018, pp. 57–82.
- [3] S. Edwards, L. Wundersitz, S. Australia, and A. Sponsored, "Distracted driving: Prevalence and motivations," pp. 1–19, 05 2019.
- [4] A. Rasouli and J. K. Tsotsos, "Joint attention in driver-pedestrian interaction: from theory to practice," *arXiv preprint arXiv:1802.02522*, 2018.
- [5] J. S. Perry and W. S. Geisler, "Gaze-contingent real-time simulation of arbitrary visual fields," *SPIE Human Vision and Electronic Imaging*, vol. 4662, pp. 57–69, 2002.
- [6] A. Morando, T. Victor, and M. Dozza, "A reference model for driver attention in automation: Glance behavior changes during lateral and longitudinal assistance," *IEEE Transactions on Intelligent Transportation Systems*, vol. 20, no. 8, pp. 2999–3009, 2019.
- [7] M. Guangyu Li, B. Jiang, Z. Che, X. Shi, M. Liu, Y. Meng, J. Ye, and Y. Liu, "Dbus: Human driving behavior understanding system," in *Proceedings of the IEEE International Conference on Computer Vision Workshops*, 2019, pp. 1–8.
- [8] Y. Xia, J. Kim, J. Canny, K. Zipser, and D. Whitney, "Periphery-fovea multi-resolution driving model guided by human attention," *arXiv preprint arXiv:1903.09950*, 2019.
- [9] J. Gaspar and C. Carney, "The effect of partial automation on driver attention: a naturalistic driving study," *Human factors*, p. 0018720819836310, 2019.
- [10] S. Jha and C. Busso, "Analyzing the relationship between head pose and gaze to model driver visual attention," in *IEEE 19th International Conference on Intelligent Transportation Systems*, 2016, pp. 2157–2162.
- [11] Z. Wan, J. He, and A. Voisine, "An attention level monitoring and alarming system for the driver fatigue in the pervasive environment," in *Brain and Health Informatics - International Conference*, 2013, pp. 287–296.
- [12] R. D. Ledesma, S. A. Montes, F. M. Poo, and M. F. Lopez-Ramon, "Measuring individual differences in driver inattention: Further validation of the attention-related driving errors scale," *Human Factors*, vol. 57, no. 2, pp. 193–207.
- [13] A. Palazzi, D. Abati, F. Solera, R. Cucchiara *et al.*, "Predicting the driver's focus of attention: the dr (eye) ve project," *IEEE Transactions on Pattern Analysis and Machine Intelligence*, vol. 41, no. 7, pp. 1720–1733, 2019.
- [14] Y. Xia, D. Zhang, J. Kim, K. Nakayama, K. Zipser, and D. Whitney, "Predicting driver attention in critical situations," in *Asian Conference on Computer Vision*, 2018, pp. 658–674.

- [15] W. Wang, J. Shen, J. Xie, M.-M. Cheng, H. Ling, and A. Borji, "Revisiting video saliency prediction in the deep learning era," *IEEE Transactions on Pattern Analysis and Machine Intelligence*, 2019.
- [16] T. Deng, K. Yang, Y. Li, and H. Yan, "Where does the driver look? top-down-based saliency detection in a traffic driving environment," *IEEE Transactions on Intelligent Transportation Systems*, vol. 17, no. 7, pp. 2051–2062, 2016.
- [17] T. Deng, H. Yan, L. Qin, T. Ngo, and B. Manjunath, "How do drivers allocate their potential attention? driving fixation prediction via convolutional neural networks," *IEEE Transactions on Intelligent Transportation Systems*, 2019.
- [18] J. Fang, D. Yan, J. Qiao, J. Xue, H. Wang, and S. Li, "DADA-2000: can driving accident be predicted by driver attention? analyzed by A benchmark," in *IEEE Intelligent Transportation Systems Conference*, 2019, pp. 4303–4309.
- [19] C. Koch and S. Ullman, "Shifts in selective visual attention: Towards the underlying neural circuitry," *Hum Neurobiol*, vol. 4, no. 4, pp. 219–227, 1985.
- [20] L. Itti, "Automatic foveation for video compression using a neurobiological model of visual attention," *IEEE Transactions on Image Processing*, vol. 13, no. 10, pp. 1304–1318, 2004.
- [21] S. S. Kruthiventi, K. Ayush, and R. V. Babu, "Deepfix: A fully convolutional neural network for predicting human eye fixations," *IEEE Transactions on Image Processing*, vol. 26, no. 9, pp. 4446–4456, 2017.
- [22] L. Jiang, M. Xu, T. Liu, M. Qiao, and Z. Wang, "Deepvs: A deep learning based video saliency prediction approach," in *Proceedings of the European Conference on Computer Vision*, 2018, pp. 602–617.
- [23] A. Borji, "Saliency prediction in the deep learning era: An empirical investigation," *arXiv preprint arXiv:1810.03716*, 2018.
- [24] W. Wang, Q. Lai, H. Fu, J. Shen, and H. Ling, "Salient object detection in the deep learning era: An in-depth survey," *CoRR*, vol. abs/1904.09146, 2019.
- [25] K. Chan, "Saliency detection in video sequences using perceivable change encoded local pattern," *Signal, Image and Video Processing*, vol. 12, no. 5, pp. 975–982, 2018.
- [26] N. Souly and M. Shah, "Visual saliency detection using group lasso regularization in videos of natural scenes," *International Journal of Computer Vision*, vol. 117, no. 1, pp. 93–110, 2016.
- [27] C. Chen, G. Wang, C. Peng, X. Zhang, and H. Qin, "Improved robust video saliency detection based on long-term spatial-temporal information," *IEEE Transactions on Image Processing*, vol. 29, pp. 1090–1100, 2019.
- [28] T. Alshawi, Z. Long, and G. AlRegib, "Unsupervised uncertainty estimation using spatiotemporal cues in video saliency detection," *IEEE Transactions on Image Processing*, vol. 27, no. 6, pp. 2818–2827, 2018.
- [29] S. Mathe and C. Sminchisescu, "Actions in the eye: Dynamic gaze datasets and learnt saliency models for visual recognition," *IEEE Transactions Pattern Analysis and Machine Intelligence*, vol. 37, no. 7, pp. 1408–1424, 2015.
- [30] P. K. Mital, T. J. Smith, R. L. Hill, and J. M. Henderson, "Clustering of gaze during dynamic scene viewing is predicted by motion," *Cognitive Computation*, vol. 3, no. 1, pp. 5–24, 2011.
- [31] Q. Lai, W. Wang, H. Sun, and J. Shen, "Video saliency prediction using spatiotemporal residual attentive networks," *IEEE Transactions on Image Processing*, vol. 29, pp. 1113–1126, 2019.
- [32] Y. Xia, "Driver eye movements and the application in autonomous driving," Ph.D. dissertation, UC Berkeley, 2019.
- [33] D. Wang, X. Hou, J. Xu, S. Yue, and C.-L. Liu, "Traffic sign detection using a cascade method with fast feature extraction and saliency test," *IEEE Transactions on Intelligent Transportation Systems*, vol. 18, no. 12, pp. 3290–3302, 2017.
- [34] S. J. Zabihi, S. M. Zabihi, S. S. Beauchemin, and M. A. Bauer, "Detection and recognition of traffic signs inside the attentional visual field of drivers," in *IEEE Intelligent Vehicles Symposium*, 2017, pp. 583–588.
- [35] D. Abati, A. Porrello, S. Calderara, and R. Cucchiara, "Latent space autoregression for novelty detection," in *Proceedings of the IEEE Conference on Computer Vision and Pattern Recognition*, 2019, pp. 481–490.
- [36] Y. Xie, L. F. Liu, C. H. Li, and Y. Y. Qu, "Unifying visual saliency with hog feature learning for traffic sign detection," in *Proceedings of IEEE Intelligent Vehicles Symposium*, 2009, pp. 24–29.
- [37] D. Wang, X. Hou, J. Xu, S. Yue, and C. Liu, "Traffic sign detection using a cascade method with fast feature extraction and saliency test," *IEEE Transactions on Intelligent Transportation Systems*, vol. 18, no. 12, pp. 3290–3302, 2017.
- [38] J. Schwehr and V. Willert, "Driver's gaze prediction in dynamic automotive scenes," in *IEEE International Conference on Intelligent Transportation Systems*, 2017, pp. 1–8.
- [39] A. Tawari and B. Kang, "A computational framework for driver's visual attention using a fully convolutional architecture," in *Proceedings of IEEE Intelligent Vehicles Symposium*, 2017, pp. 887–894.
- [40] A. Palazzi, F. Solera, S. Calderara, S. Alletto, and R. Cucchiara, "Learning where to attend like a human driver," in *Proceedings of IEEE Intelligent Vehicles Symposium*, 2017, pp. 920–925.
- [41] S. Vora, A. Rangesh, and M. M. Trivedi, "Driver gaze zone estimation using convolutional neural networks: A general framework and ablative analysis," *IEEE Transactions on Intelligent Vehicles*, vol. 3, no. 3, pp. 254–265, 2018.
- [42] F.-H. Chan, Y.-T. Chen, Y. Xiang, and M. Sun, "Anticipating accidents in dashcam videos," in *Proceedings of Asian Conference on Computer Vision*, 2016, pp. 136–153.
- [43] Y. Yao, M. Xu, Y. Wang, D. J. Crandall, and E. M. Atkins, "Unsupervised traffic accident detection in first-person videos," *arXiv preprint arXiv:1903.00618*, 2019.
- [44] Y. Kang, H. Yin, and C. Berger, "Test your self-driving algorithm: An overview of publicly available driving datasets and virtual testing environments," *IEEE Transactions on Intelligent Vehicles*, vol. 4, no. 2, pp. 171–185, 2019.
- [45] J. Redmon and A. Farhadi, "Yolov3: An incremental improvement," *arXiv*, 2018.
- [46] L. Chen, G. Papandreou, F. Schroff, and H. Adam, "Rethinking atrous convolution for semantic image segmentation," *CoRR*, vol. abs/1706.05587, 2017.
- [47] M. Cordts, M. Omran, S. Ramos, T. Rehfeld, M. Enzweiler, R. Benenson, U. Franke, S. Roth, and B. Schiele, "The cityscapes dataset for semantic urban scene understanding," in *Proceedings of the IEEE Conference on Computer Vision and Pattern Recognition*, 2016, pp. 3213–3223.
- [48] Z. Li, T. Motoyoshi, K. Sasaki, T. Ogata, and S. Sugano, "Rethinking self-driving: Multi-task knowledge for better generalization and accident explanation ability," *arXiv preprint arXiv:1809.11100*, 2018.
- [49] A. Zhao, T. He, Y. Liang, H. Huang, G. V. d. Broeck, and S. Soatto, "Lates: Latent space distillation for teacher-student driving policy learning," *arXiv preprint arXiv:1912.02973*, 2019.
- [50] X. Huang, C. Shen, X. Boix, and Q. Zhao, "Salicon: Reducing the semantic gap in saliency prediction by adapting deep neural networks," in *Proceedings of the IEEE International Conference on Computer Vision*, 2015, pp. 262–270.
- [51] J. Pan, C. Canton-Ferrer, K. McGuinness, N. E. O'Connor, J. Torres, E. Sayrol, and X. Gir'o i Nieto, "Salgan: Visual saliency prediction with generative adversarial networks," *CoRR*, vol. abs/1701.01081, 2017.
- [52] M. Cornia, L. Baraldi, G. Serra, and R. Cucchiara, "A deep multi-level network for saliency prediction," in *2016 International Conference on Pattern Recognition*, 2016, pp. 3488–3493.
- [53] K. Zhang and Z. Chen, "Video saliency prediction based on spatial-temporal two-stream network," *IEEE Transactions on Circuits and Systems for Video Technology*, vol. 29, no. 12, pp. 3544 – 3557, 2019.